Scientific Contributions Oil & Gas, Vol. 48. No. 4, December: 463 - 487

SCIENTIFIC CONTRIBUTIONS OIL AND GAS

Testing Center for Oil and Gas
LEMIGAS

Journal Homepage:http://www.journal.lemigas.esdm.go.id
ISSN: 2089-3361, e-ISSN: 2541-0520

Structural Configuration And Paleogeography of The "Krishna" Field in The Sunda Basin

Kharis Surya Wicaksana[1], Dumex Pasaribu[1], Humbang Purba[2]

[1]Department of Geology Engineering, Faculty of Exploration and Production Technology, Universitas PERTAMINA, Simprug, South Jakarta 12220, Indonesia

[2]Research and Development Center for Oil and Gas Technology "LEMIGAS", Ciledug Raya Street No. 109, Kebayoran Lama District, South Jakarta City, 12230, Indonesia

Corresponding Author : Kharis Surya Wicaksana (kharissuryawicaksana@gmail.com)

Manuscript received: October 27th, 2025; Revised: November 17th, 2025
Approved: December 08th, 2025; Available online: December 30th, 2025; Published: December 30th, 2025.

ABSTRACT - The Krishna Field is located in the Sunda Basin and is estimated to have significant hydrocarbon potential. This study aims to analyze the subsurface conditions, geological structure configuration, and paleogeography of the field. The research utilizes 3D seismic data and drilling well data obtained from the Research and Development Center for Oil and Gas Technology "LEMIGAS". The methodology for this study comprises several stages, namely the preparation stage**,** which involves a literature review and the process of acquiring supporting data. The data processing stage includes well-seismic tie, well correlation, horizon and fault picking, and the generation of structural and isopach maps. The analysis stage, in which the processed data is analyzed through electrofacies analysis, sequence stratigraphy, seismic stratigraphy, and depositional environment analysis. The results of the study indicate that during the pre-rift phase, the basement rocks were faulted by northeast-southwest trending normal faults with a dominant dip to the southeast, forming a half-graben basin structure. The Talang Akar Formation was deposited in a transitional environment as a syn-rift phase deposit. This was followed by a transgression event, marked by a rise in sea level, where the Baturaja Formation was deposited as a late syn-rift phase deposit, and subsequently followed by the Gumai Formation during the post-rift phase, which has a consistent layer thickness but a more complex and intense structure, deposited in a shallow marine environment.

Keywords: Structure, half-graben, paleogeography, Sunda Basin.

How to cite this article:

Kharis Surya Wicaksana, Dumex Pasaribu, Humbang Purba 2025, Structural Configuration And Paleogeography of The "Krishna" Field in The Sunda Basin, Scientific Contributions Oil and Gas, 48 (4) pp. 463 - 487. DOI org/10.29017/scog.v48i4.1964.

INTRODUCTION

In the development of oil and gas fields, the exploration stage is crucial for analyzing geological conditions and mapping the presence of hydrocarbons. This phase provides valuable insights for minimizing risks and understanding the distribution of key elements.

The research focused on the "Krishna" Field and its location in the UTM 48 S zone, covering an area of approximately 116.25 km^2. The "Krishna" Field is situated in the Sunda Basin, which is connected to the Asri Basin. These basins are structurally separated by the Seribu Heights, located in the westernmost part of the North West Java Basin. Both basins are part of a series of back-arc basins in Sumatra and the Java Sea and are also identified as rift basins distinct from the North West Java Basin (Reminton 1985; Todd & Pulunggono 1971).

The Sunda Basin exhibits promising hydrocarbon potential, as evidenced by 25 years of production. This production originates from 21 potential accumulations, or 200 exploration wells, yielding a success rate of approximately 10%. The average production is 9,000 barrels of oil per day (BOPD), with an estimated total of approximately 800 million barrels of hydrocarbons. PT CNOOC SES Ltd. is one of the companies responsible for managing this area and conducting exploration and exploitation activities in the Asri Basin within a field block in Southeast Sumatra (Wight et al., 1986).

To improve production in the Sunda Basin, it is essential to acquire a more comprehensive understanding of the subsurface geology, particularly in the "Krishna" Field. Our objective is to examine the geological structure and paleogeographic conditions of the reservoir and cap rocks within the Talang Akar Formation, Baturaja Formation, and Gumai Formation in the research area. It is essential to note that our study relies on analysis of 3D seismic data and information from five wells, with a focus on horizon analysis, geological structures, and the paleogeography of both the reservoir and the overburden within the specified formations. Basin development and sedimentary facies distribution in Indonesian basins are closely related to regional tectonic evolution, making paleogeographic reconstruction an essential approach for understanding depositional systems and basin architecture (Lelono, 2022). This research aims to identify the distribution of the Talang Akar, Baturaja, and Gumai Formations, as well as the geological structures in the area. Additionally, it will involve analyzing the paleogeographic conditions and depositional environments, which could be beneficial for further analyses, including common risk segment (CRS) mapping.

Regional physiography

According to Reminton (1985) and Todd & Pulunggono (1971), the North West Java Basin comprises multiple sub-basins, including the Sunda Basin and the Asri Basin. These sub-basins are categorized as part of the back-arc basin and are not considered part of the rift basin.

Recent geological studies classify the Asri Basin as a pull-apart basin, which originated at the southern end of a significant regional strike-slip fault system (Ralanarko et al., 2020; Siringo-ringo, 2025). Similarly, the Sunda Basin, often analyzed alongside the Asri Basin, exhibits characteristics indicative of pull-apart tectonics dating back to the Early Paleogene in Sundaland. This aligns with the concepts of extrusion tectonics proposed by Tapponier et al (1982), which led to wrench faulting in the Sundaland region.

Furthermore, this pattern is consistent with the Tertiary basins in the recent back-arc of Sumatra, which are predominantly formed by a wrench fault system that generates pull-apart grabens, as observed in the North and Central Sumatra Basin (Pasaribu et al., 2025). Further research is required in the Sunda and Asri Basins to confidently elucidate the wrench and pull-apart tectonic systems present in this region. Understanding these dynamics is essential for effective exploration and production strategies in the region.

The Sunda Basin is located at the southeastern tip of the Eurasian Plate and is part of the Sunda Microplate (Figure 1). The basin is bordered by the Seribu Platform structure, which features a northeast-trending fault plane that separates the

Sunda Basin from the Arjuna Sub-basin. To the southwest, the basin is delineated by the Lampung Plateau. To the south, it is bounded by the South Sumatra Basin, while to the north, it extends into the Sunda Shelf, lying beyond the Java Sea. In the northeastern section of the Sunda Basin, the Asri Sub-basin is bordered by the Seribu High (Bishop, 2000). Clements and Hall (2007) reported that tectonic activity initiated during the Late Cretaceous and Paleocene, involving subduction along the southern margin of the Eurasian Plate, extending from southern Sumatra to the Meratus Mountains.

This process was succeeded by the collision of fragments from the Gondwana Continent with the southern part of the Eurasian Plate, likely resulting in a shift in subduction direction towards the west-east. Consequently, this led to the rise of various sections of the Sunda Shelf as continental areas. The tectonic evolution and regional structure outlined by Clements and Hall (2007) can be effectively illustrated through the tectonic framework of Sundaland presented by Metcalfe (2017) (see Figure 2).

During the Eocene, there was a reduction in the frequency of collisions between fragments of Gondwana and the Eurasian Plate. Currently, subduction in the southern part of Java remains active, resulting in west-east oriented extension and the development of a relatively north-south trending graben (Clements & Hall 2007). Bishop (2000) notes that in the Oligocene, the rate at which the Australian and Indian Plates moved northward also diminished, leading to the formation of a complex half graben on the Sunda Shelf at its northern edge.

At the onset of the Neogene, a new subduction zone emerged in southern Java, which remains active today. The compressional tectonics that have been present since the Neogene have altered the tectonic patterns established in earlier periods, resulting in a new orientation that is more west-east, in parallel with the existing subduction patterns.

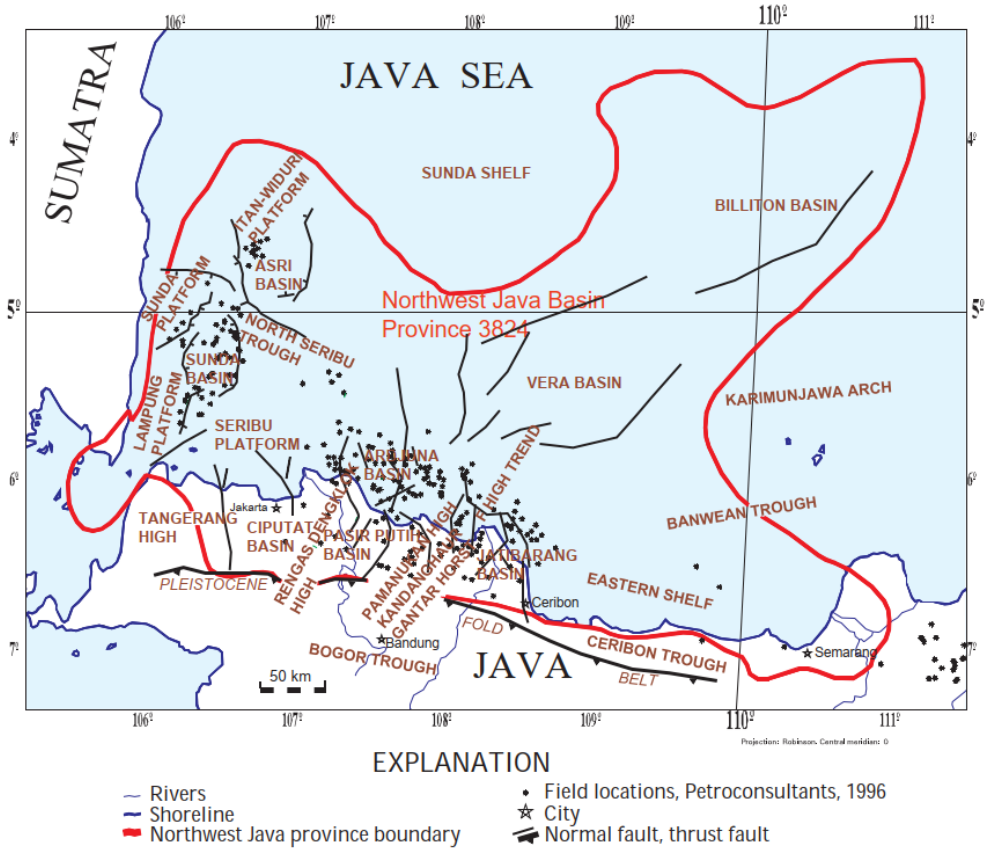

Figure 1. The geological structure of the boundary of the North West Java Basin Province is clearly detailed in Bishop (2000).

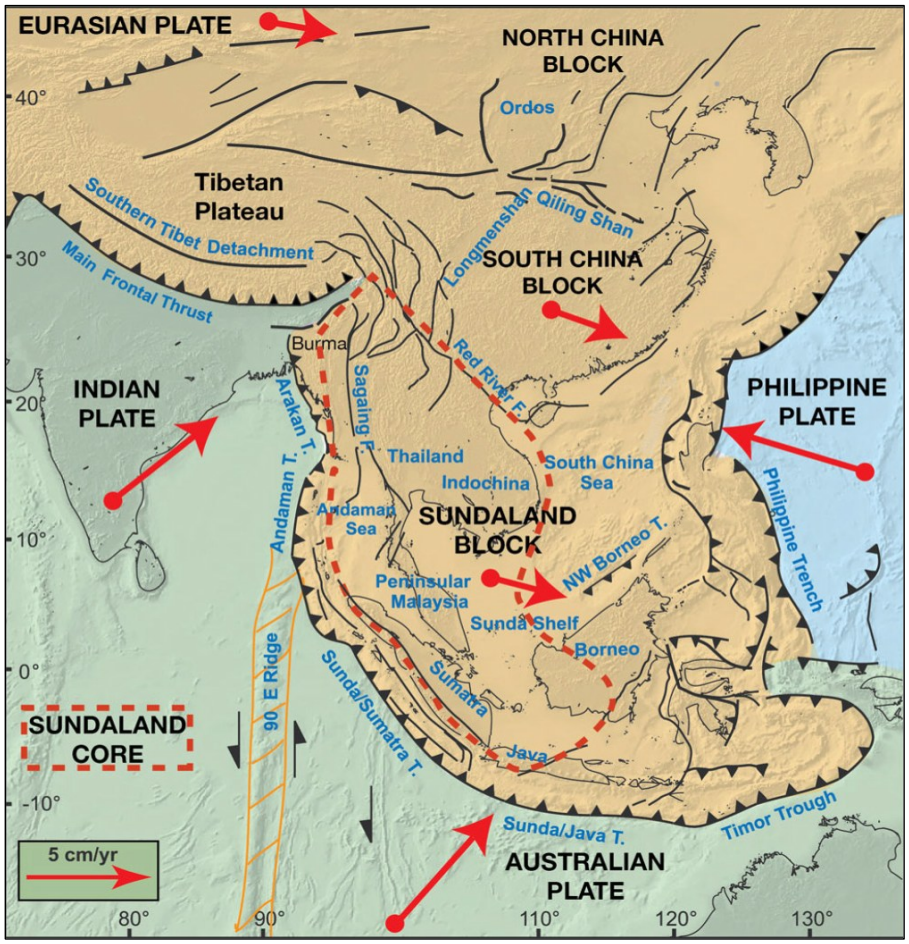

Figure 2. Tectonic framework of Sundaland (Metcalfe, 2017)

The existing fault system is part of the Sumatran fault system, characterized by faults oriented north-northeast in the Sunda Strait. Along the southeastern coast of Sumatra, there are north-south-oriented faults, including the Kepayang Fault, which intersects with the Lampung high. In West Java, wrench faults with a northeast-southwest orientation (N70°E) can also be observed (Wight et al., 1986).

Structural Geology

According to Wight et al. (1986), the geological structure of the Sunda Basin is characterized by grabens and half-grabens that predominantly dip to the east. These formations result from north-south rifting that extends northeastward, particularly in the Sunda Shelf area. The primary fault system in this region produces isolated grabens and substantial half-grabens, oriented between N45°W and N40°E, as shown in Figure 3.

Wight et al. (1986) observed that the primary fault system in this basin consists of a north-south trending normal fault that extends approximately 64 km in length. The rotational movement of the island of Sumatra shapes the structural formations within the Sunda Basin. Notably, during the Oligocene, there was a significant shift in plate convergence from a northward orientation to its current orientation, approximately between N26°E and N38°E. This change is thought to have played a key role in the development of these normal faults.

In addition, several faults are oriented northwest-southeast. These faults traverse both the basement and the overlying sedimentary deposits, establishing boundaries for sedimentation centers. During the Oligocene period, the graben and half-graben formations underwent subsidence, becoming focal points for sedimentation in the Sunda Basin. The largest and deepest sedimentation center is the

Seribu graben, which contains accumulations of continental sediment from the Banuwati and Talang Akar Formations (Wight et al., 1986).

Regional stratigraphy

The stratigraphy of the Sunda Basin (Figure 4) reveals a significant sea level rise from the Banuwati to Gumai Formation, followed by a decrease from the Air Benakat Formation to Cisubuh. This description is based on multiple preceding studies by Aldrich et al. (1995), Todd & Pulonggono (1971), and Wight et al. (1986), which generally arrange formations from oldest to youngest as follows:

- **Basement (early – late cretaceous)**

  The oldest rock discovered in the basin consists of low-grade metamorphic formations, including schist, gneiss, and quartzite. This assemblage also features two varieties of igneous rocks: intrusive igneous rocks, such as granite and granodiorite, and extrusive igneous rocks, including basalt, andesite, and trachyte (Koesoemadinata 2004).

- **Banuwati formation (late eocene - early ligocene)**

  The formation is deposited unconformably on the basement and consists of continental sedimentary lithologies, including lacustrine clay sediments, alluvial fans, and fluvial deposits (Aldrich et al., 1995). It comprises non-marine sediments that document transgressive events in lacustrine environments. The shale and mudstone serve as the primary source rock, while the sandstone may function as a reservoir layer.

- **Talang akar formation (late oligocene - early miocene)**

  Deposited unconformably above the basement and conformably above the Banuwati Formation, this layer formed during the marine transgression phase. It consists of lithology resulting from fluvial processes, with the lower section comprising interbedded claystone and coarse clastic sandstone, which has the potential to serve as a reservoir (Todd & Pulunggono 1971). At the top, this formation consists of interbedded mudstone and coal, overlain by several layers of sandstone formed by fluvio-

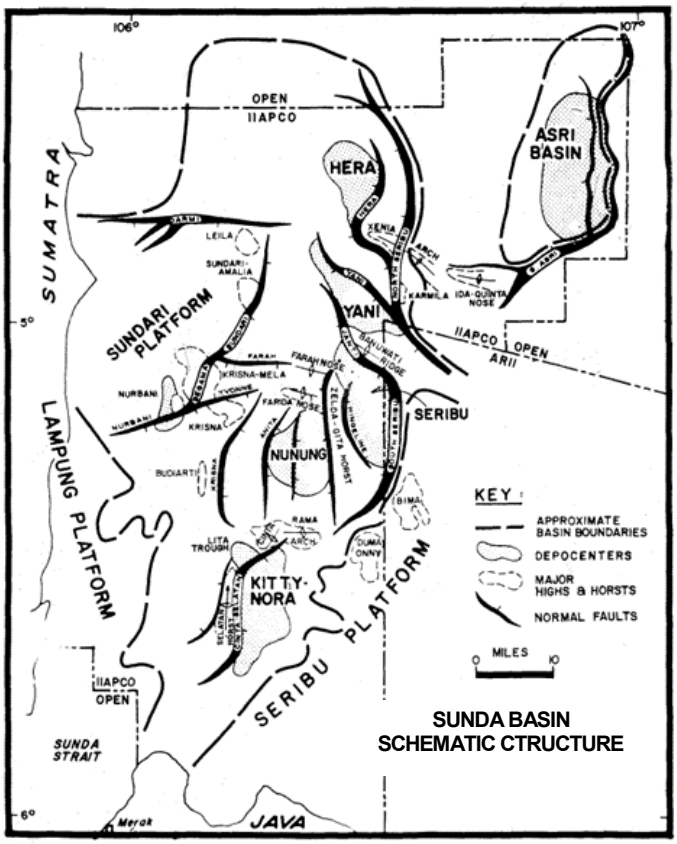

Figure 3. Schematic map of the structure of the Sunda - Asri Basin (Wight et al., 1986)

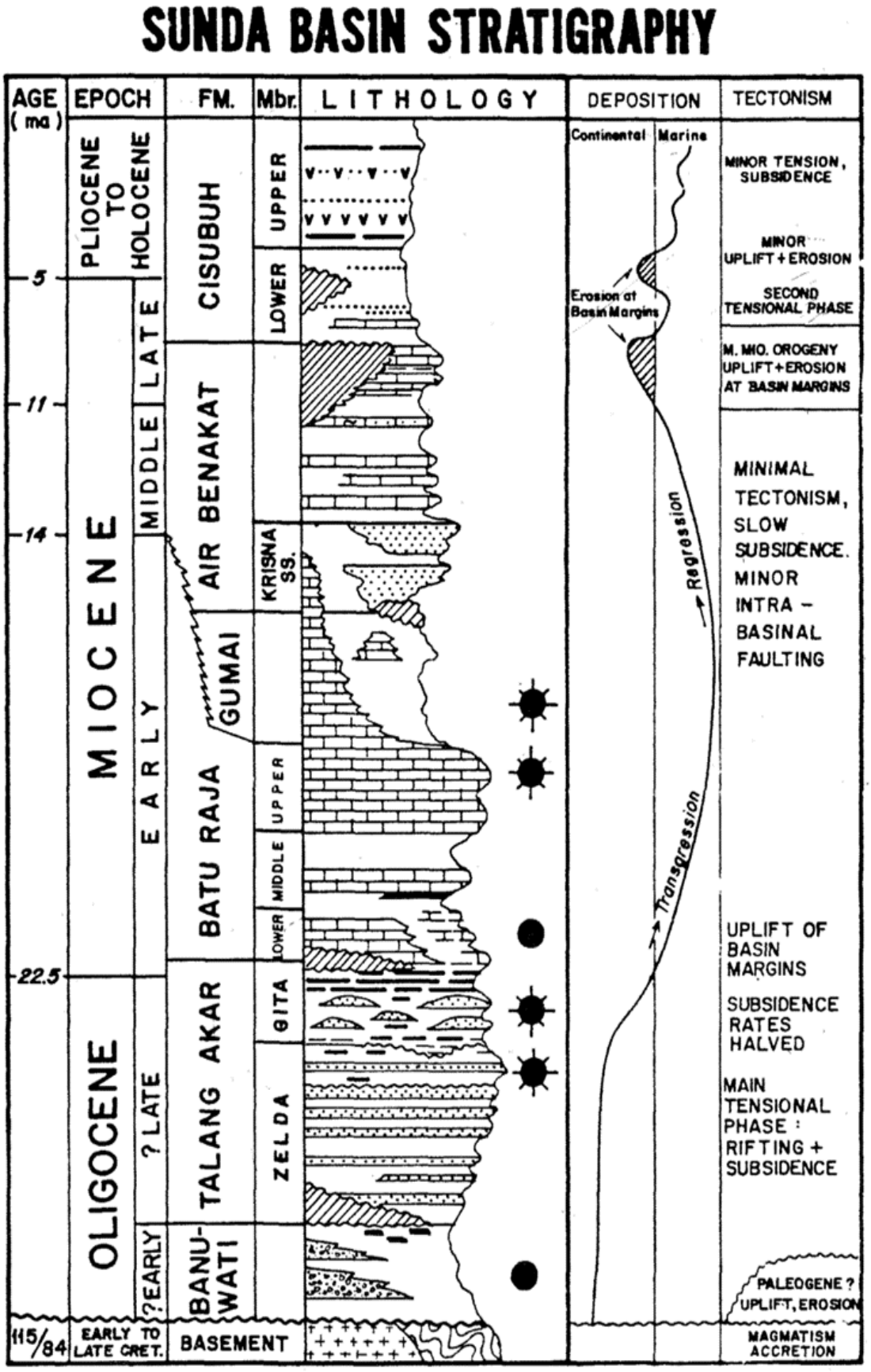

Figure 4. Regional stratigraphy of the Sunda Basin (Wight et al., 1986)

deltaic processes. Additionally, there are sediment inserts with carbonate characteristics, suggesting that the upper section of this formation was deposited in non-marine to marginal marine environments. The sandstone lithology in this formation serves as a reservoir rock, while the shale and claystone may function as a secondary source rock.

- **Baturaja formation (early miocene)**

  Deposited conformably atop the Talang Akar Formation, this formation predominantly features reef carbonate lithology, bank limestone, lime mud, and mudstone at its base, all of which were formed during the transgression phase in a lower delta plain environment. This process led to the development of shallow marine facies limestone, characterized by shelf limestone at the bottom and bioclastic reef limestone at the top, which is typical of Indonesian carbonate reservoirs (Widarsono 2011).

- **Gumai formation (early miocene)**

  The Gumai Formation, which can attain a thickness of up to 410 meters, was deposited conformably atop the Baturaja Formation. It emerged during a period of maximum marine transgression and is characterized primarily by gray shale lithology in an inner-middle-shelf environment. This formation comprises mudstone, shale, limestone, and mudstone interbedded with silt and sand. Notably, the mudstone within this formation serves as a caprock (Wight et al., 1986).

METHODOLOGY

The research methodology utilized in this study begins with a well seismic tie, which involves aligning well data with seismic data to establish a reference marker for horizon delineation. Following this, well data is correlated to gain insight into the distribution of lithology within the formation. An electrofacies analysis is then performed using gamma ray (GR) and spontaneous potential (SP) log data, when available, to identify stratigraphy, facies, and their relationships with the depositional environment of each well. This process includes examining the patterns of the GR or SP curves and correlating them with the relative stratigraphic cross-section model to produce a GDE map (as illustrated in Figure 5).

Stratigraphic sequence analysis incorporates electrofacies analysis to provide insights into the patterns of facies changes identified in the Log GR curve. These variations offer valuable information about the sea level changes recorded in the well. Furthermore, seismic sequence analysis is performed to identify reflection terminations, which serve as sequence boundaries, as well as to analyze the reflection configurations that occur between these boundaries.

The process of seismic stratigraphic analysis entails examining seismic sequences to identify reflection terminations as sequence boundaries and to characterize the configurations of reflections between these boundaries. This analysis also delineates horizons and faults using 3D seismic data, thereby facilitating understanding of the distribution and boundaries of various layers. Additionally, it allows for the assessment of structures that intersect these layers by evaluating the continuity of the reflectors.

A structure map is generated using the horizon data obtained in the previous processing stage. This involves a time-to-depth conversion process to create a detailed map illustrating the geological structure and subsurface morphology of the research area.

Creating isopach maps helps analyze geological history. This involves calculating the disparity between two surfaces, from the upper sequence boundary to the lower boundary. Isopach maps are instrumental in analyzing paleogeographical conditions, as they help interpret the accommodation space for sediment deposition in a given area.

Depositional environmental analysis involves interpreting the distribution of depositional environmental facies based on previous assessments. This process results in a depositional environment map, also known as a GDE Map,

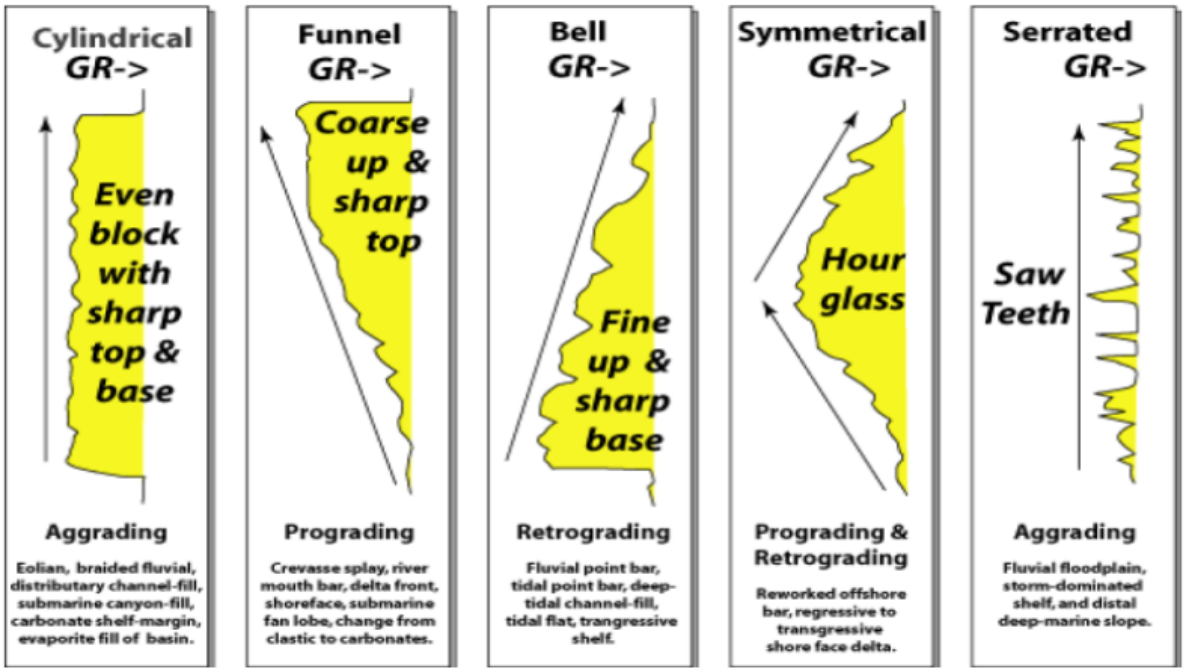

(a)

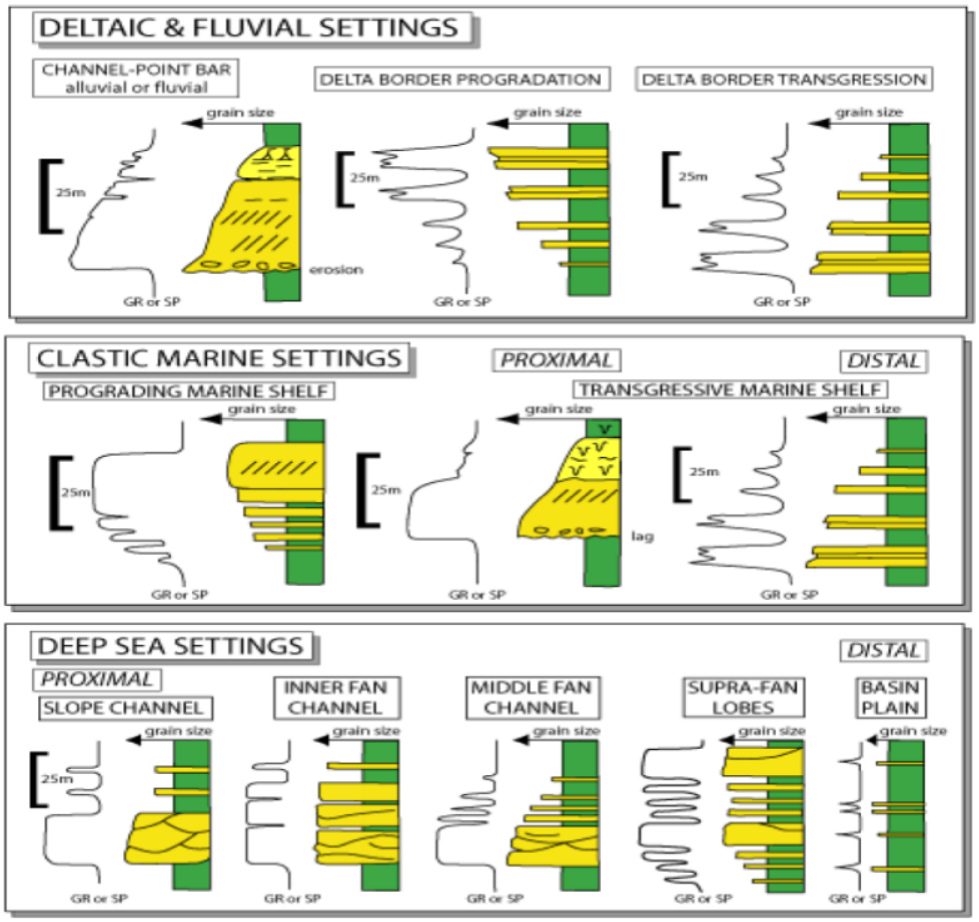

(b)

Figure 5. Characteristics of GR and SP well logs, which indicate grain size and depositional environment (Kendall, 2005)

which visually represents the distribution of facies that define a depositional environment in the study area.

RESULT AND DISCUSSION

Well Seismic Tie

Seismic data and well data are captured in different domains; specifically, seismic data is represented in the time domain, measured in milliseconds (ms), whereas well data is presented in the depth domain, measured in feet (ft). Consequently, it is essential to integrate these datasets. This integration process requires converting well data into the time domain using checkshot and sonic data. The primary objective of this stage is to ensure the accurate positioning of each marker boundary or sequence boundary within the seismic data. This procedure was performed across five wells, and the results are detailed in Table 1.

Table 1. Results of the well seismic tie process from the five wells.

Well	Maximum correlation	Time shift (ms)
Kappa_12	0.780	0
Alpa_01	0.809	-2
Kappa_01	0.763	0
Beta_01	0.804	2
Kappa_10	0.846	0

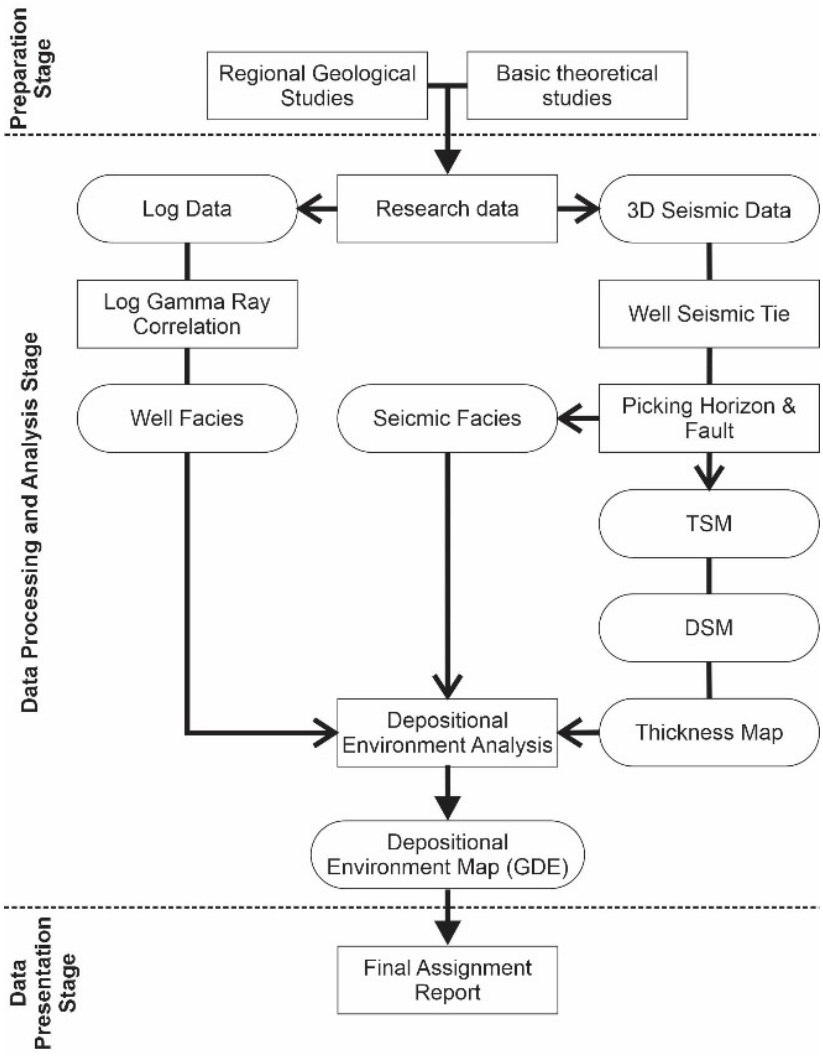

Figure 6. Flow diagram of the research.

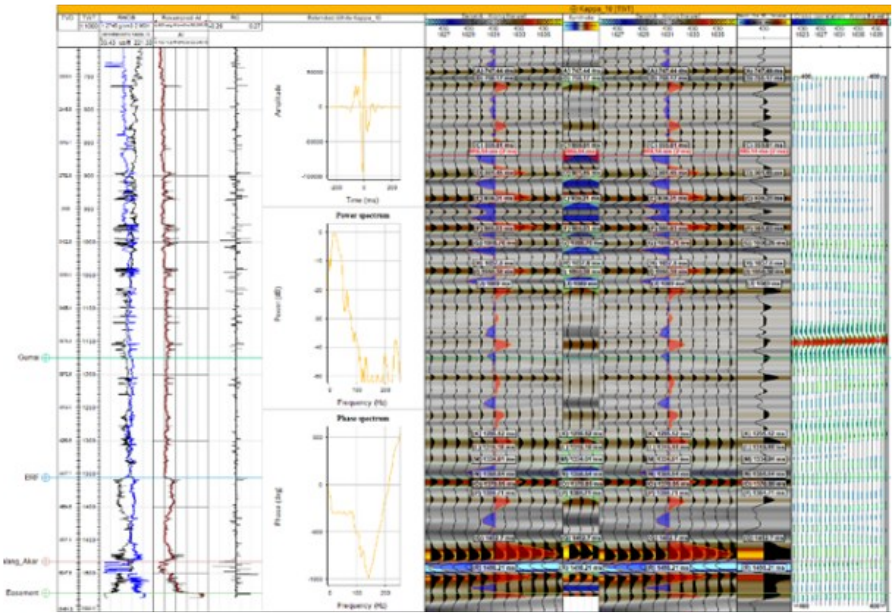

Figure 7. The results of the synthetic seismogram for the well seismic tie at the Kappa 10 well are good, as indicated by the aligned red bands.

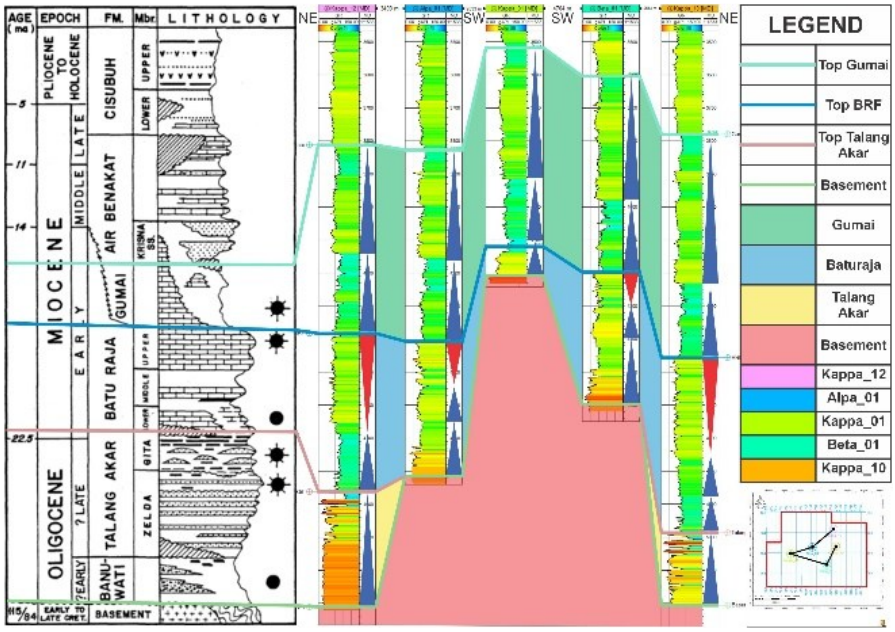

Figure 8. Well correlation uses well data in the well section display.

According to Table 1, the outcomes are promising, as they demonstrate maximum correlation exceeding 0.5, with time shifts of less than 20 ms and near 0 ms. The wavelet used adopts a deterministic approach and incorporates the extended white algorithm within the Petrel software (see Figure 7).

Well correlation

The correlation analysis utilizes five well data points in the following order: Kappa_12, Alpha_01, Kappa_01, Beta_01, and Kappa_10, which are oriented in a northeast-southwest direction. Additionally, seismic data is integrated to trace the continuity of sequence boundaries or formations in each well, aligning with the direction of the seismic reflector. The objective of this analysis is to determine the distribution patterns of the formations and geological structures between the wells.

According to the marker data (see Figure 8), the deepest point of the top basement, interpreted as a

high area, is located in the Kappa_01 well at a depth of 1282.44 m. In contrast, the lowest elevations are found in the Kappa_12 and Kappa_10 wells, at depths of 1588.27 m and 1586.65 m, respectively. The top of the Talang Akar formation was not encountered in the Alpa_01, Kappa_01, and Beta_01 wells. These data were subsequently entered and visualized in the Petrel application. Well correlation was also performed using seismic data, yielding Figure 9.

The analysis indicates that the basement is classified as a pre-rift megasequence type. Additionally, the Talang Akar Formation is recognized as an early syn-rift deposit that overlies the basement. In contrast, the Baturaja Formation is characterized as a late syn-rift deposit that extends beyond the basement. The thickness variations between these two formations are attributed to their capacity to fill the depocenter, which is influenced by basin topography and structural features. Finally, the Gumai Formation is recognized as a post-rift deposit because its sediment thickness is relatively uniform compared with that of the preceding formations.

Seismic interpretation

In the realm of seismic interpretation, the chosen seismic section, commonly referred to as herolines, has been identified and generated to illustrate the basin conditions within the research area. These heroline tracks are oriented perpendicular to the present geological structures. It is important to note that the predominant orientation of the geological structures in the research area is NE–SW, which results in the heroline trajectories aligning NW–SE.

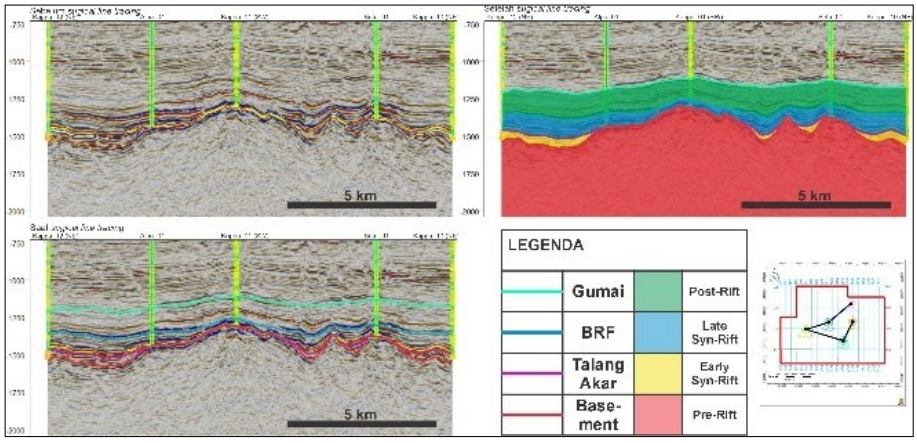

Figure 9. Well correlation interpretation uses seismic data with a NE – SW orientation.

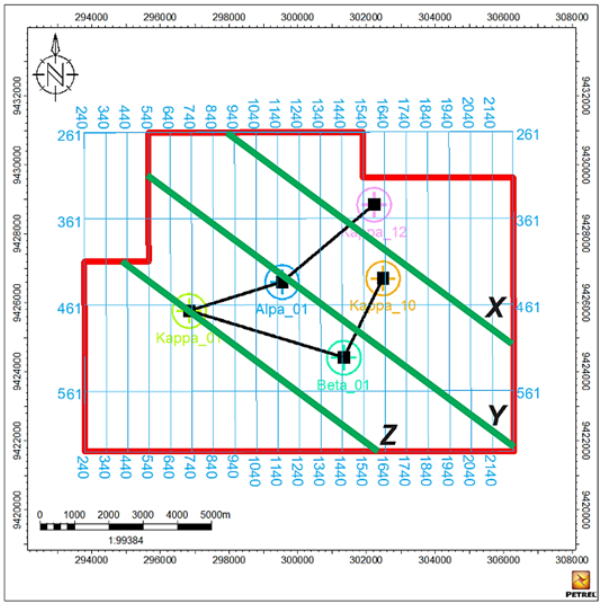

Figure 10. Location of Heroline X, Y, and Z trajectories

Three heroline trajectories are mapped as depicted in Figure 10. Based on seismic data analysis, the research area can be categorized into four types of deposits: pre-rift, early syn-rift, late syn-rift, and post-rift. This classification is based on the thickness of the layers and the presence of structures that influence their deposition.

- **Heroline X**

  This heroline is situated farthest north among the herolines and has a track length of approximately 10 km. It is also in proximity to the Kappa_12 and Kappa_10 wells (Figure 11). Horizon interpretation is conducted by drawing and connecting markers or sequence boundaries between adjacent wells, carefully following the continuity of the seismic reflector's direction. In contrast, fault interpretation involves identifying discontinuities in the seismic reflector that may indicate vertical displacement associated with faults. The interpretation results presented in Figure 11 indicate that the northwestern region is characterized by elevated terrain, while the southeastern region is a lowland area. In the southeastern part, there is a prominent downward fault structure that dips relatively eastward. Additionally, another fault structure exhibits a descending orientation, with a predominant dip direction toward the southeast.

- **Heroline Y**

  The heroline is positioned among the other herolines along a track that stretches approximately 13 km. This path runs past the Alpa_01 well and lies adjacent to the Beta_01 well (refer to Figure 12). Horizon interpretation is conducted by delineating and connecting markers or sequence boundaries between neighboring wells, following the continuity of the seismic reflectors. In contrast, fault

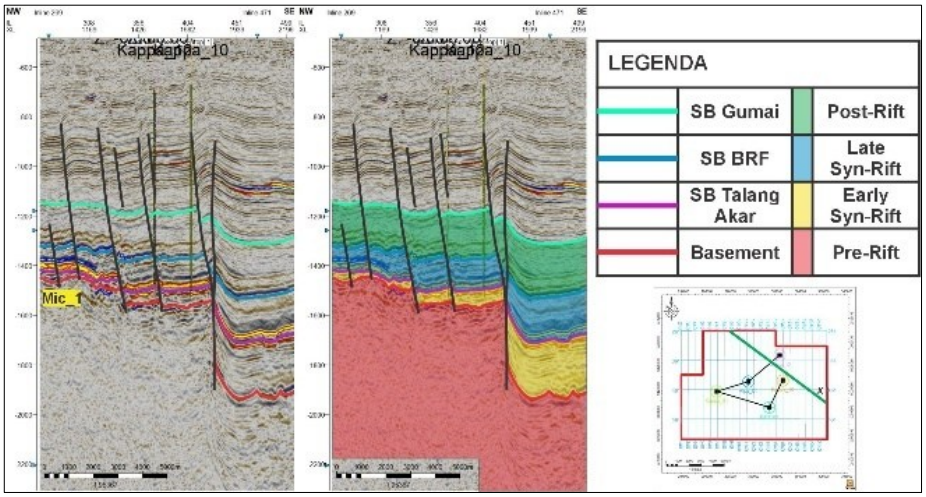

Figure 11. Seismic interpretation results on Heroline X, y-axis in the time domain

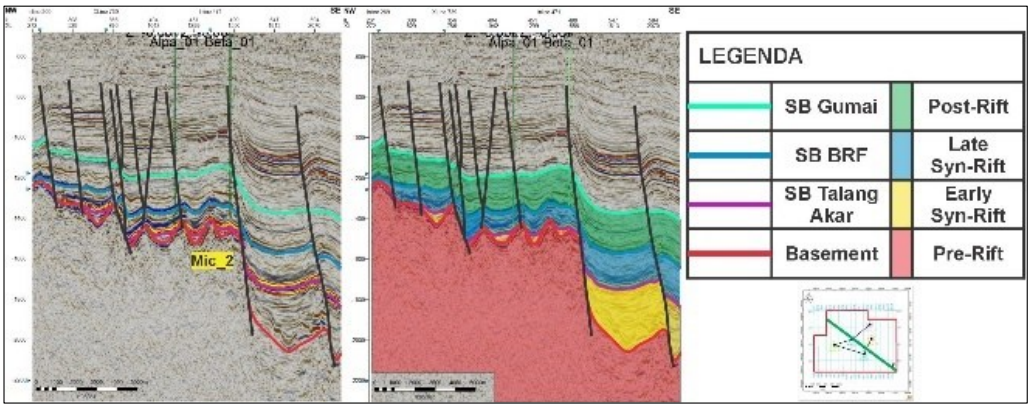

Figure 12. Seismic interpretation results on Heroline Y, y-axis in the time domain

interpretation involves identifying discontinuities in seismic reflectors that may indicate fault movement, either upward or downward. According to the interpretation results presented in Figure 12, the northwestern region is characterized by high elevations, whereas the southeastern portion is identified as a lowland. There are three significant descending fault structures located in the northwest and southeast, all exhibiting a relative dip direction toward the southeast.

- **Heroline Z**

  This Heroline is the furthest south among the Herolines and has an approximate track length of 9 km. The path intersects with the Kappa_01 well (see Figure 13). Horizon interpretation involves plotting and connecting markers or sequence boundaries between adjacent wells by tracing the continuity of the seismic reflector's direction. In contrast, fault interpretation focuses on identifying discontinuities in the seismic reflector that fault-related vertical movements may influence. The interpretation results presented in Figure 13 indicate that the northwestern region is characterized by elevated terrain. The central area also exhibits high morphological features, while the southeastern part is predominantly low-lying.

  Two significant downward-fault structures are identified in the northwest and southeast, both exhibiting a relative dip toward the southeast. To the west of the southeastern major descending fault, there exists another descending fault that dips in the opposite direction, creating a horst in its central portion.

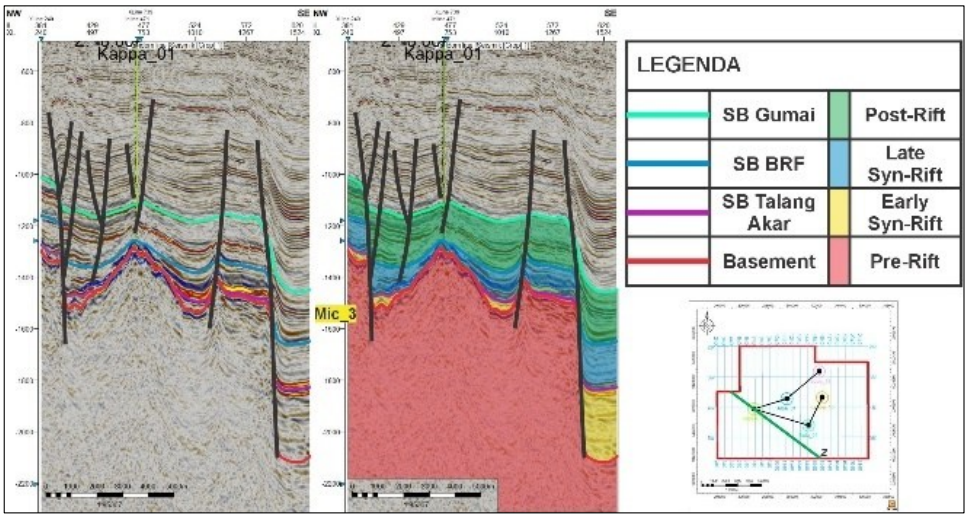

Figure 13. Seismic interpretation results on Heroline Z, y-axis, in the time domain.

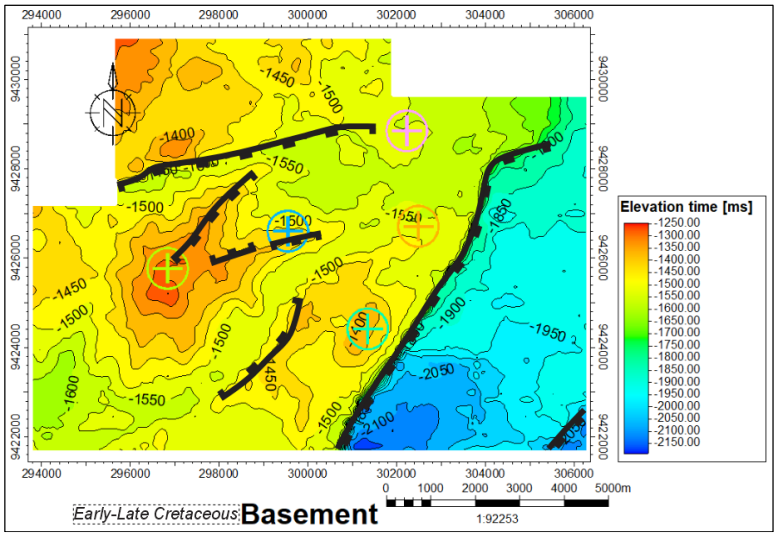

Figure 14. Top Basement time structure map (Early – Late Cretaceous)

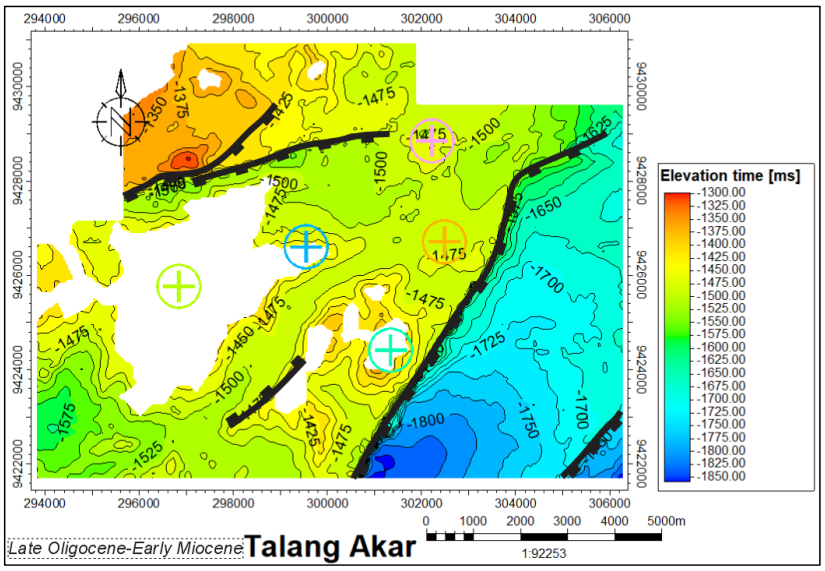

Figure 15. Top Talang Akar Formation time structure map (Late Oligocene – Early Miocene)

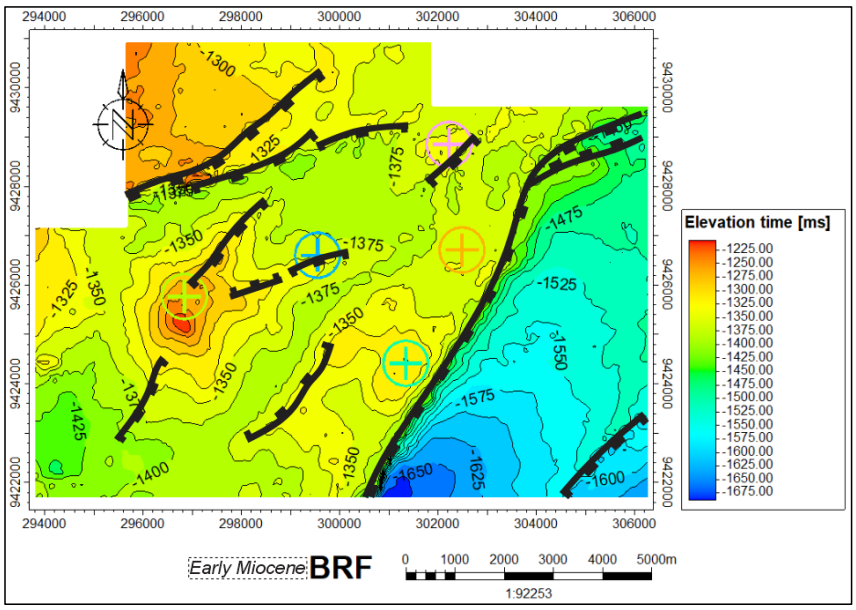

Figure 16. Top Baturaja Formation time structure map (Early Miocene)

A half-graben has likely formed in the sedimentary deposits at the base of the high area, extending toward the elevated regions.

Time Structure Map

This contour map is based on the results of seismic interpretation for each horizon in the time domain (in milliseconds). It provides insights into the presence of geological structures, as evidenced by the observed contour patterns. In this study, we present four time-structure maps for each horizon, detailed as follows.

- **Top Basement (Early – Late Cretaceous)**

  Figure 14 illustrates the distribution of data within the time frame of -1250 ms to -2150 ms. This map reveals a geological structure characterized by normal faults that formed during the extensional phase, predominantly oriented northeast-southwest. The morphology of elevated areas is also evident on this map. In the southeastern section, a prominent low area is distinguished, which is separated from the higher region in the northwest by a significant downward fault.

- **Top talang akar formation (late oligocene – early miocene)**

  Figure 15 presents a map illustrating the distribution of data for the time window -1300 ms to -1850 ms. This map reveals a geological structure characterized by normal faults that developed during an extensional phase, predominantly oriented in a northeast-southwest direction. In the southeastern region, there is a depression that is distinctly separated from the higher area in the northwestern section by a significant downward fault. The white areas on the map indicate regions where sedimentary deposits from this formation are onlapping onto the existing elevated areas and hills. This horizon is believed to correspond to early syn-rift deposits, as it exhibits a structural pattern closely resembling that of the top basement, with sediment sources migrating from north to south.

- **Top Baturaja formation (early miocene)**

  Figure 16 presents a map illustrating the distribution of data for the time range -1225 ms to -1675 ms. This map reveals a geological structure characterized by normal faults that are becoming increasingly complex and pronounced, having formed during the extensional phase with a predominant northeast-southwest orientation. In the southeastern region, there is a lower area, distinctly separated from the higher region to the northwest by a significant downward fault. This horizon is believed to represent part of the late syn-rift deposits. The elevation in the interior regions appears to be gradually becoming shallower, particularly in the low areas where sedimentary deposits are accumulating, while the morphology of the higher areas remains evident on this map.

- **Top gumai formation (early miocene)**

  Figure 17 presents a map illustrating the distribution of data from the time range of −1075 ms to −1450 ms. The map reveals geological structures characterized by normal faults that exhibit a complex, intense configuration resulting from an extensional phase with a predominant northeast-southwest orientation. The southeastern region is depicted as a lower area, distinctly separated from the higher terrain in the northwest by a significant downthrown fault. This horizon is interpreted as part of the late post-rift deposits. In the deeper zones, the topography appears to become shallower, particularly in low-lying areas that serve as depositional sites, where mountainous features are no longer visible or have been transformed into hilly terrain.

Depth structure map

This map was generated using a time-to-depth conversion in Petrel, specifically the velocity model feature. The model parameters employed are V = V0 = Vint, where V0 denotes the well TDR at the surface. This research encompasses four horizons, resulting in the following map.

- **Top basement (early – late cretaceous)**

  This map illustrates the distribution of data within a depth range of -4000 ft to -7000 ft. It reveals the presence of geological structures characterized by normal faults that formed during the extensional phase, with a predominant northeast-southwest orientation. Additionally, the map depicts the morphology of a high region, whereas the southeast area is identified as a low region, delineated from the high area in the northwest by a significant downward fault (Figure 18).

- **Top talang akar formation (late oligocene – early miocene)**

  This map illustrates the distribution of data within a depth range of -4100 ft to -5850 ft. The geological structural pattern observed closely resembles that of the upper basement. In the southeastern region, there exists a low area that is distinctly separated from the high area to the northwest by a significant downward fault. The white area depicts a high region where the Talang Akar Formation is absent and is recognized as a source rock

locale. This horizon is interpreted as part of the early syn-rift deposits. It is estimated that the sediment originates from the north and flows toward the south, emanating from the high area within this region (Figure 19).

- **Top Baturaja formation (early miocene)**

  This map illustrates the distribution of data within a depth range of -3900 ft to -5550 ft. The geological structure depicted exhibits normal faults that are evolving into more complex and intense forms, which originated during an extensional phase characterized by a predominant northeast-southwest trend. In the southeastern section, there is a low area, clearly delineated by a major downward fault from the higher region to the northwest.

  This horizon is likely associated with late syn-rift deposits, with sediments originating from the elevated areas in the north. The elevation within the interior regions appears to be progressively shallower, particularly in the low areas where sedimentary deposits are accumulating. This is especially evident in the high area morphology, which is becoming

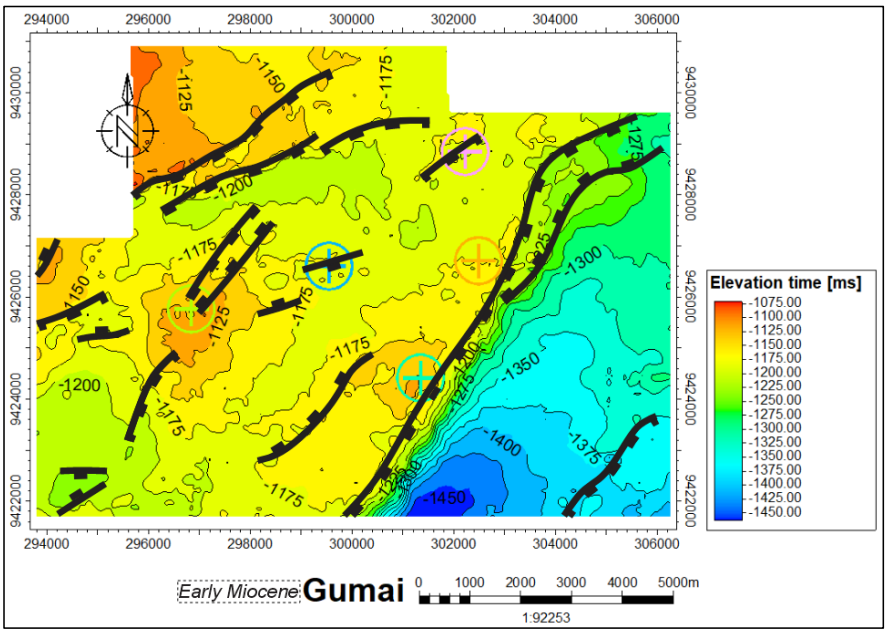

Figure 17. Top Gumai Formation time structure map (Early Miocene)

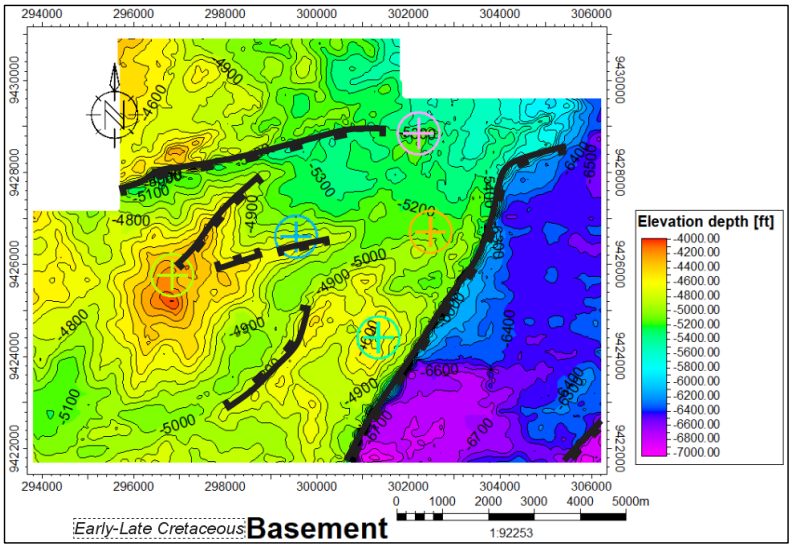

Figure 18. Top basement depth structure map (Early – Late Cretaceous)

increasingly buried (Figure 20).

- **Top Gumai Formation (Early Miocene)**

  This map illustrates the distribution of data within a depth range of -3450 ft to -4450 ft. It reveals a geological structure characterized by a network of more complex and pronounced normal faults that developed during the extensional phase and predominantly orient northeast-southwest. In the northwestern part of the map, there is an elevated area separated from a low-lying region by a significant downward fault. This horizon is believed to represent part of the post-rift deposits.

  The surface of the horizon appears more inclined, particularly in the lower areas where sedimentary deposits have accumulated. The morphology of the elevated region is less distinct and has been transformed into a hill, as depicted in this map (Figure 21).

Isopach Map

This map presents the vertical distribution of a formation unit's thickness within the depth domain (ft). In this study, two reservoir zones have been identified: the Talang Akar Formation and the Baturaja Formation. Consequently, an isopach map has been produced as detailed below.

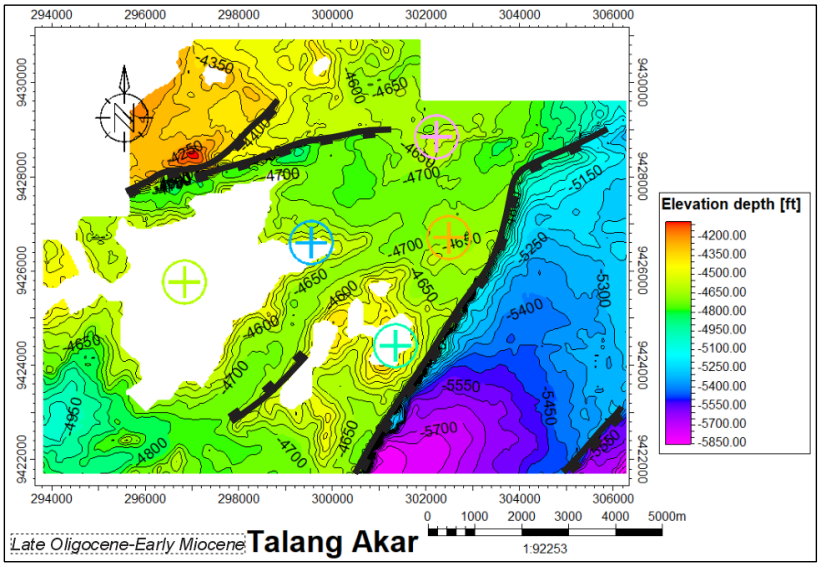

Figure 19. Top Talang Akar Formation depth structure map (Late Oligocene – Early Miocene)

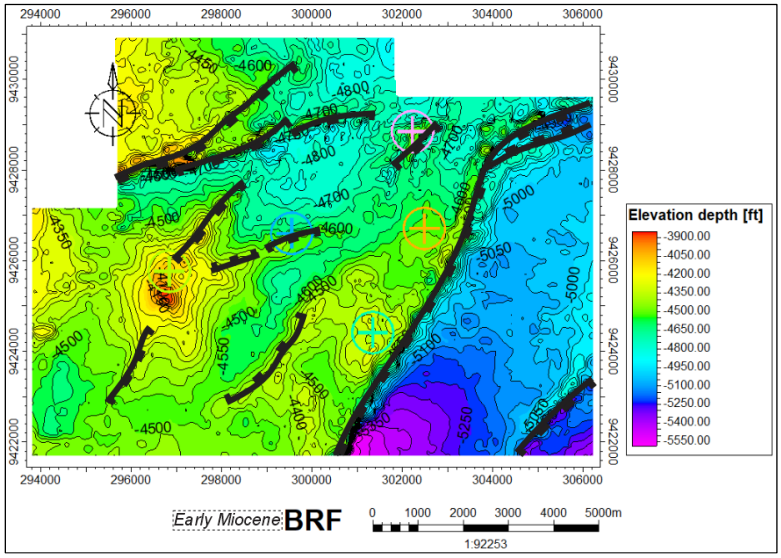

Figure 20. Top Baturaja Formation depth structure map (Early Miocene)

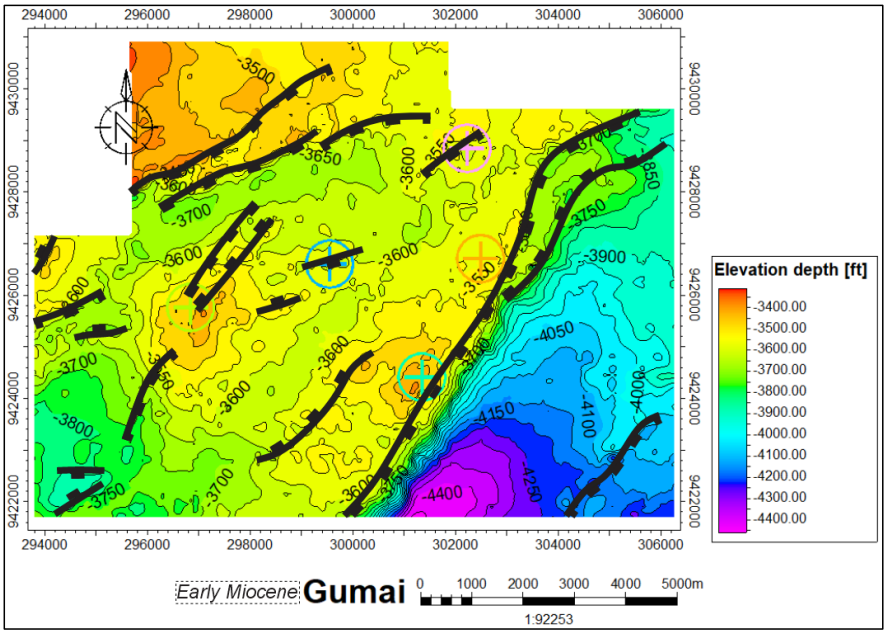

Figure 21. Top Gumai Formation depth structure map (Early Miocene)

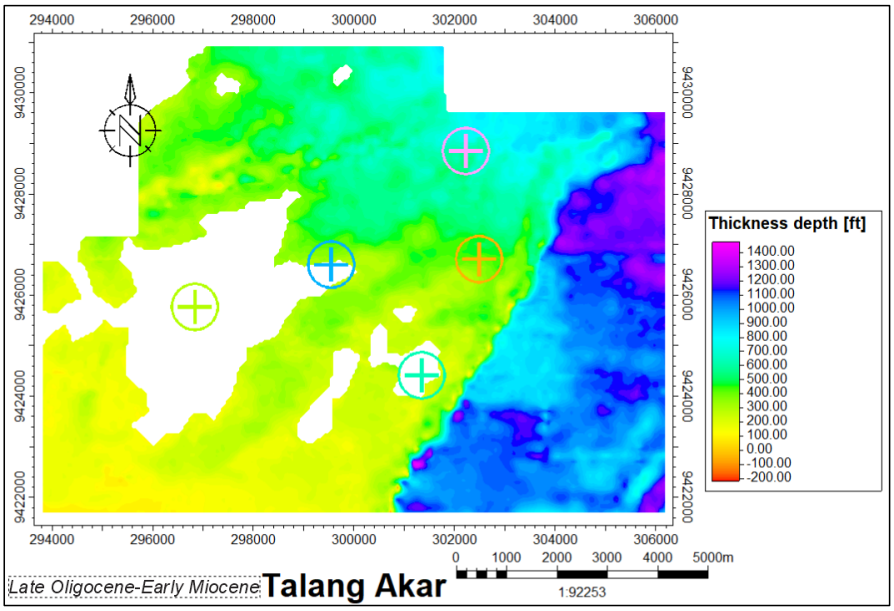

Figure 22. Talang Akar isopach map

- **Talang akar formation**

  The isopach map of the Talang Akar Formation illustrates the vertical distribution of rock layer thickness between the basement surface and the horizon of the Talang Akar Formation. The thickness of these layers ranges from 0 to 1,400 feet (see Figure 22). The thickest sections are found in the eastern to southeastern areas, while thinner layers are more prevalent in the western to southwestern regions. Notable thickness variations can help identify fault locations, thereby providing insight into the characteristics of early syn-rift deposits.

- **Baturaja formation**

  The isopach map of the Baturaja Formation illustrates the distribution of vertical rock layer thicknesses extending from the Baturaja surface to the horizon of the Talang Akar Formation and the underlying basement. The thickness of these layers ranges from 0 to 800 feet (Figure 23). The thickest

sections are found in the southern to southeastern regions, while thinner areas are located in the northern to northwestern sections, particularly in high terrain and hilly regions. The sedimentary deposits within this formation are aligned with increasing elevation, corresponding to variations in depth toward the southeast, and are interpreted as late syn-rift deposits.

Facies analysis

- **Well facies Analysis**

The facies grouping in this analysis is based on well gamma-ray (GR) logs. This is assessed through characteristic patterns, electrofacies recognitions, and their similarities with findings from earlier researchers, allowing for an accurate representation of facies associations. Such associations provide a more comprehensive understanding of the depositional environment. The identification of the facies model in this study is based on the work of previous researchers, specifically Rider (1999) and Omoboriowo et al. (2012), focusing on rocks with sandstone lithology. The results of the facies association analysis, along with a more detailed examination of the reservoir layers derived from five well log data from the research area, are presented in Table 2.

Table 2 shows that there are two depositional environmental systems in the research area, namely the transition area depositional environmental system, which consists of the delta and shore environments, and the shallow marine system, which consists of the shelf. The delta depositional environment is categorized into three facies associations. The first, lacustrine (LK-1), is characterized by an aggradational depositional pattern comprising alternating claystone and sandstone layers. The second association, the delta plain (DP-1), features a rough upward pattern interspersed with clay-rich rocks.

Lastly, the delta front (DF-1) displays a smooth upward trend, with a transition in lithology from sand to clay rock. The delta depositional environment is categorized into three facies associations. The first, lacustrine (LK-1), is characterized by an aggradational depositional pattern comprising alternating claystone and sandstone layers. The second association, the delta plain (DP-1), features a rough upward pattern interspersed with clay-rich rocks. Lastly, the delta front (DF-1) displays a smooth upward trend, with a transition in lithology from sand to clay rock.

In shallow marine systems, namely in the shelf depositional environment, it is divided into two facies associations, namely the offshore bar facies association (OB-1), characterized by a sandstone-dominated depositional pattern, which shows less shale content, and offshore shale (OS-1), characterized by a shale-dominated depositional pattern. Next, a correlation of the results of the GR log analysis was carried out at each marker depth in the five wells to determine the distribution of facies associations or GDE, for example, as in Figure 24.

- **Seismic facies analysis**

This analysis classifies sedimentary facies associations based on seismic image reflector patterns and characteristics that reflect a depositional environment association. The researchers used Roksandic (1978) as a reference for the grouping. The results of the facies association grouping are presented in Table 3.

Table 3 illustrates three distinct facies associations within the research area, reflecting depositional environments ranging from the Talang Akar to the Gumai Formations. These associations include delta facies in Mic-1, shore facies in Mic-2, and shelf facies in Mic-3. This analysis is conducted for each area to delineate the boundaries of the various depositional environments. The facies distribution is also mapped based on the seismic reflectors identified along the previously established heroline. For instance, Figure 25 below presents the locations of seismic sampling and the delineation of depositional environment boundaries.

Depositional environment analysis

The determination of the gross depositional environment (GDE map) is derived from the integration of well facies and seismic facies, supported by previously constructed structure maps and isopach maps. The GDE map is based on the Talang Akar, Baturaja, and Gumai formations, and the paleogeographic evolution interpreted in this study is consistent with previous studies from Indonesian basins, which demonstrate that

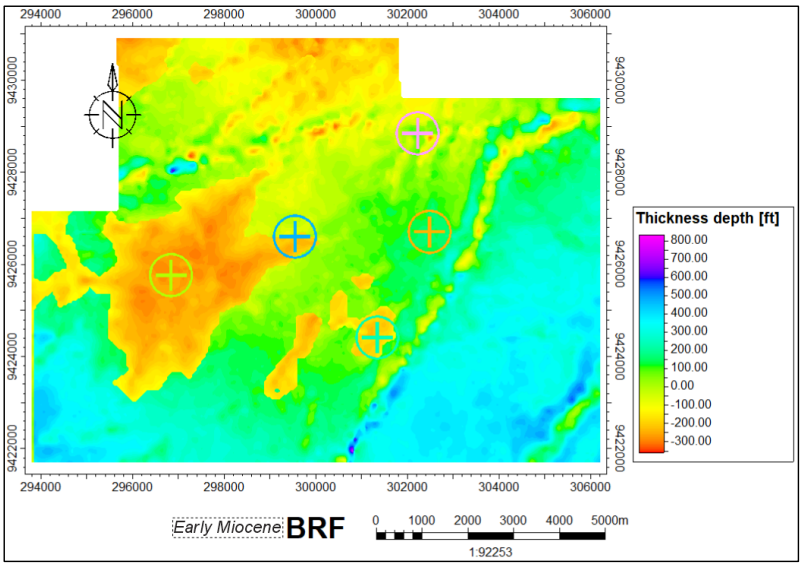

Figure 23. Baturaja isopach map

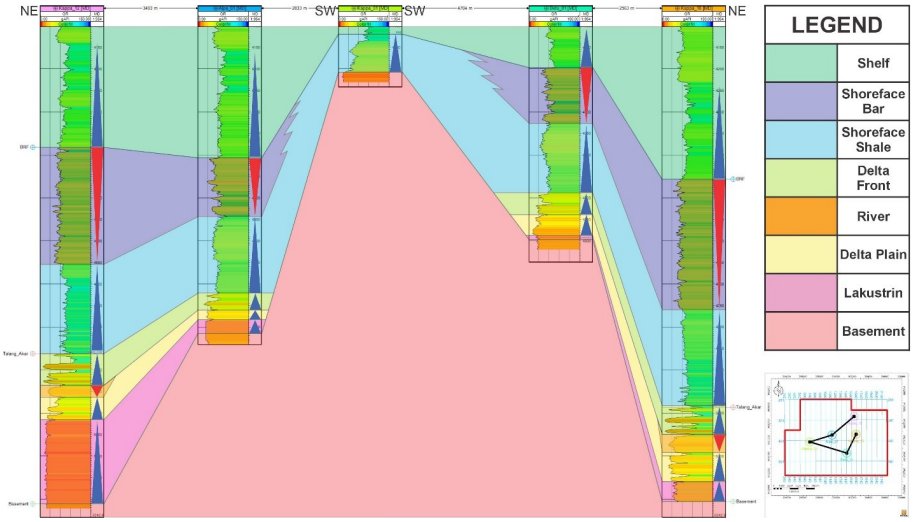

Figure 24. Correlation of well facies associations within each well

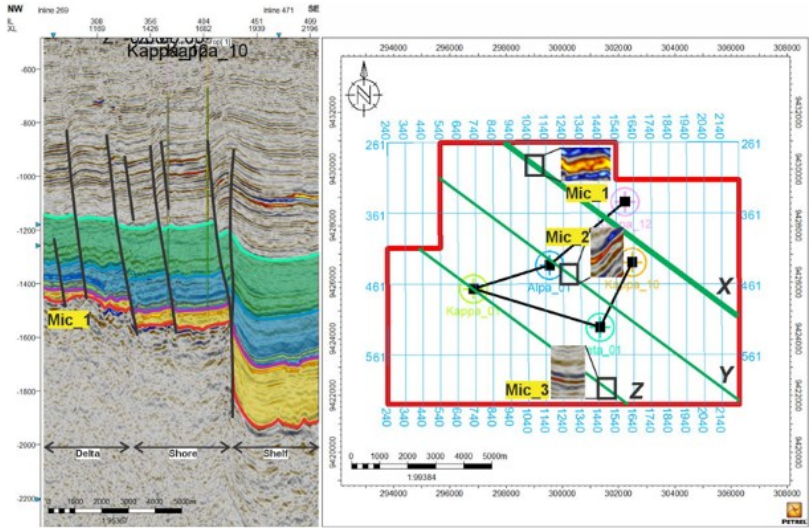

Figure 25. Distribution of Heroline X seismic facies associations

Table 2. Results of well facies association grouping

Facies code	GR log	Electro-facies	Facies association model	Interpretation	Facies association	Depositional environment
LK-1	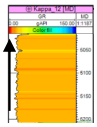	Serrated	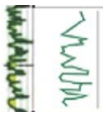 Omoboriowo et al., (2012)	It has an aggradation deposition pattern, interbedded between claystone and sandstone	Lacustrine	Delta
DP-1	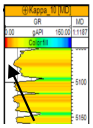	Funnel	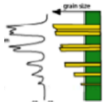 Rider (1999)	It has a coarse upward pattern, interspersed with clay rock	Delta Plain	
DF-1	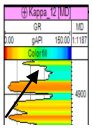	Bell	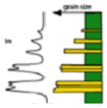 Rider (1999)	It has a fine upward pattern with a change in lithology from sand to clay rock	Delta Front	
SB-1	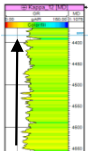	Blocky	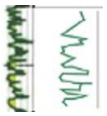 Omoboriowo et al., (2012)	It has an aggradation pattern dominated by sandstone intercalated with clay	Shoreface Bar	Shore
SS-1	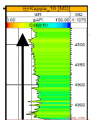	Blocky	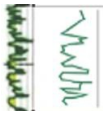 Omoboriowo et al., (2012)	It has a gradation pattern dominated by mudstone intercalated with sandstone	Shoreface Shale	
OB-1	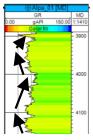	Symme-trical	 Omoboriowo et al., (2012)	It has a sedimentation pattern that is dominated by sandstone. Shows decreasing shale content	Offshore Bar	Shelf
OS-1	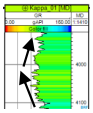	Symme-trical	 Omoboriowo et al., (2012)	It has a depositional pattern that is dominated by shale. Shows increasing shale content	Offshore Shale	

Table 3. Results of seismic facies determination

Facies code	Seismic imagery	Internal configuration	Reflector continuity	Amplitude intensity	Interpretation	Facies association
Mic-1	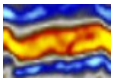	Parallel	Continue	High	It has high settling energy and a large sediment supply	Delta
Mic-2		Divergent	Continue	High	It has high deposition energy which settles in areas with steep slopes	Shore
Mic-3	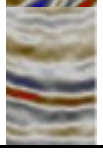	Parallel	Continue	Moderate	It has moderate settling energy on sloping surfaces	Shelf

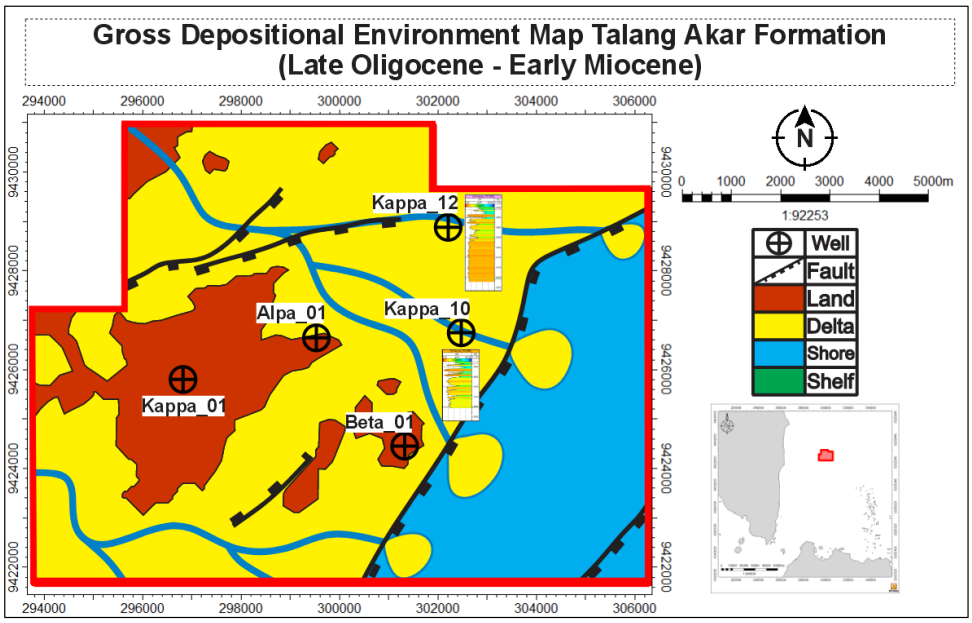

Figure 2. Depositional environment map of the Talang Akar Formation (Late Oligocene – Early Miocene)

depositional environments commonly deepen basinward in response to tectonic controls and sequence stratigraphic development (Lelono et al., 2022). The depositional environment map of the Talang Akar Formation, dating from the Late Oligocene to Early Miocene, indicates that it was formed during the early syn-rift tectonic phase. This formation was deposited within a transitional depositional environment. The facies associations identified on this map suggest shore and deltaic settings, as evidenced by the low gamma-ray log data predominantly featuring sandstone. Additionally, seismic data reveals varying thicknesses of the formation, which are separated by faults. The landscape is characterized by high areas and hills. Toward the southeast, the depositional environment shifts to a shallow marine setting. Overall, the map suggests that the direction of deposition is oriented towards the southeast, with sediment supply originating from the northwest (Figure 26).

The following is an overview of the depositional environment of the Baturaja Formation, which dates to the upper Early Miocene and was formed during the late syn-rift tectonic phase. The accompanying map illustrates a significant transformation, revealing that sedimentary deposits have enveloped the highlands. Two distinct depositional systems are evident, transitioning from northwest to southeast, specifically from transitional to shallow marine environments. The research location indicates a deepening of these systems. This observation is further corroborated by well data analysis, particularly log data, which indicates transgression events characterized by shifts in lithological properties from coarse-grained to fine-grained rock. Additionally, seismic data reveal varying thicknesses within this formation, implying that these changes are linked to rising sea levels or transgressions. The direction of sediment supply remains consistent with prior assessments, flowing from northwest to southeast (refer to Figure 27).

Final item is the depositional environment map of the Gumai Formation, which dates back to the lower Early Miocene and was formed during the post-rift tectonic phase. This map illustrates notable changes in the depositional environment. As observed in the previous map, some regions that were once elevated have transitioned into a deep marine environment. This indicates that the transgression event, or sea level rise, persisted and peaked during this period, reaching what is known as the maximum flooding surface. This observation is further supported by well data analysis, which revealed sediment composed of fine grains, and consistent seismic data thickness across each well. The supply and direction of sedimentation remain

unchanged, flowing from northwest to southeast. Additionally, the delta depositional environment no longer plays a significant role in the study area (Figure 28). The findings of this study suggest that the structure in this region is a normal fault, characterized by graben and half-graben morphology with a northeast-southwest alignment. These results align with the research conducted by Wight et al. (1986) concerning the structural schematic map of the Sunda-Asri Basin in the Krishna Field.

Paleogeographic analysis reveals that the study area comprises two primary depositional systems: a transitional system and a shallow marine system. The transitional system includes lacustrine, delta plain, delta front, and shoreface facies, primarily located in the central to northwestern parts of the area.

In contrast, offshore facies, representing the shallow marine system, are predominantly found in the southeastern region. Sediment supply originated from the northwestern highlands, resulting in sediment dispersal from northwest to southeast toward deeper marine environments. The development of these depositional settings was closely linked to regional tectonic evolution, commencing with the pre-rift phase, followed by the early to late syn-rift phases marked by the deposition of the Talang Akar and Baturaja formations, respectively, and culminating in the post-rift phase characterized by the deposition of the Gumai Formation in a shallow marine setting, indicative of a transgressive event.

This interpretation is further supported by the regional stratigraphy of the Sunda Basin, as examined in multiple studies by Aldrich et al. (1995), Todd & Pulonggono (1971), and Wight et al. (1986). In addition, layers of the Talang Akar Formation were found to be onlapping onto the basement, which represents the morphology of the elevated area. This interpretation aligns with the findings of Todd & Pulunggono (1971), who asserted that the Talang Akar Formation was deposited unconformably atop the basement. The Gumai Formation, on the other hand, is characterized by a maximum flooding surface event, indicative of a concluding transgression phase. Log data reveal that it predominantly features high gamma ray values, suggesting that it is primarily composed of shale lithology within an inner-middle shelf environment.

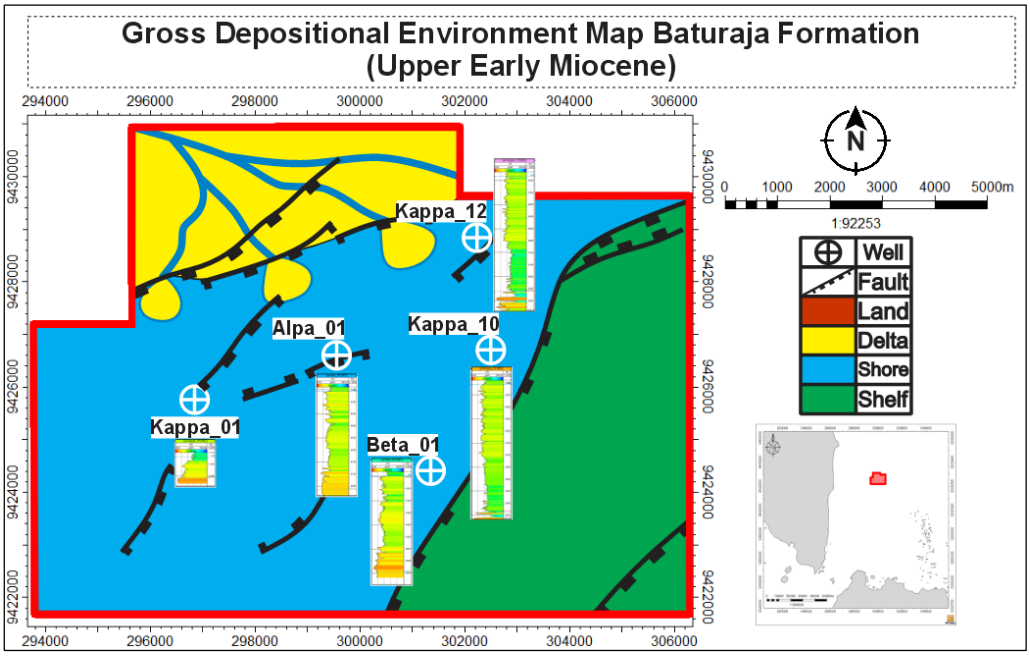

Figure 27. Depositional environment map of the Baturaja Formation (Early Upper Miocene)

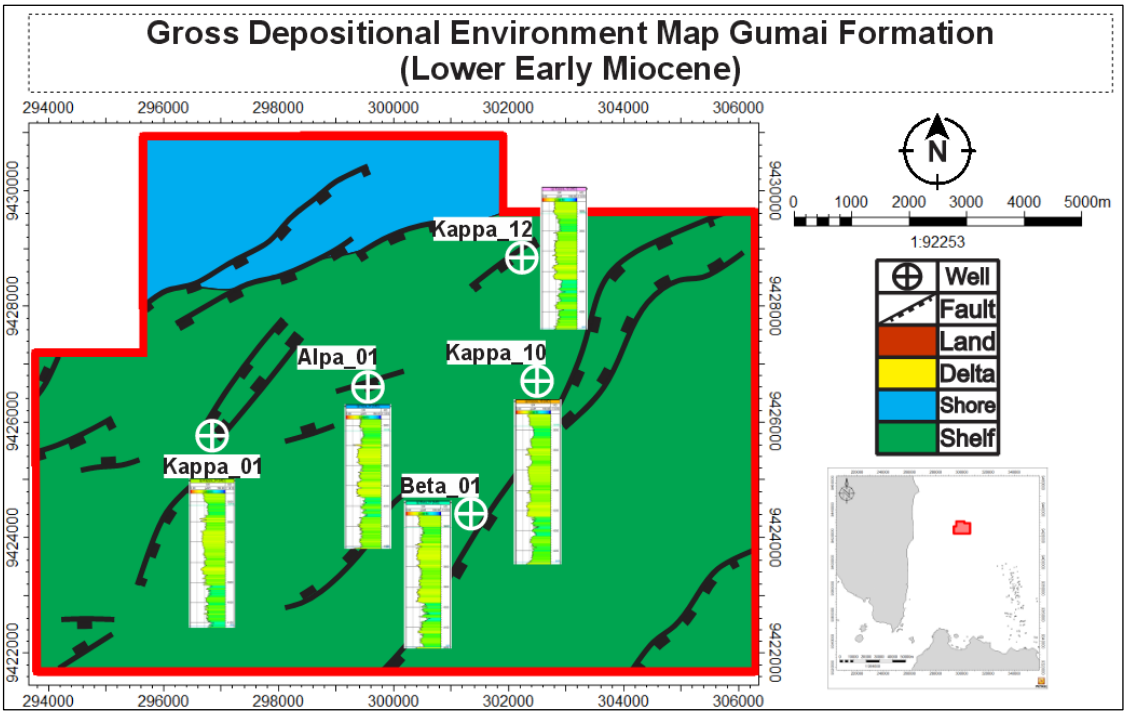

Figure 28. Depositional environment map of the Gumai Formation (Early Lower Miocene)

CONCLUSION

The geological structure observed in the research area consists of a normal fault oriented in a northeast-southwest direction, extending from the northwest to the southeast of the region. The predominant dip of the fault is directed towards the southeast. Additionally, there are faults exhibiting opposite dips, which give rise to horst and graben formations. It is believed that this fault emerged as a result of the rotational movements of Sumatra Island during the Oligocene epoch or through north-south rifting, resulting in the creation of a half-graben structure serving as a basin within the study area.

The paleogeography of the study area is characterized by two distinct depositional environmental systems: transitional areas and shallow marine systems. These environments developed during the early syn-rift, late syn-rift, and post-rift tectonic phases. Within the transitional depositional system, the facies present include lacustrine, delta plain, delta front, and shoreface facies, which are dispersed throughout the central to northwestern regions of the study area. In contrast, the shallow marine depositional system features offshore facies located in the southeastern part of the area. Sediments in this research region were supplied from the northwest, leading to a depositional direction that extends from the northwest towards the southeast, traversing high areas and transition zones before reaching the shallow marine and, ultimately, the deep marine environments.

ACKNOWLEDGEMENT

The first author wishes to extend heartfelt gratitude to God Almighty, Allah SWT, as well as to his family and relatives for their unwavering prayers and support. Special thanks are also due to Mrs. Dumex Pasaribu, and the co-author as well, for her guidance as the supervisor in the Department of Geology Engineering, Faculty of Exploration and Production Technology, University of PERTAMINA, and to BBPMGB LEMIGAS for providing the opportunity to conduct research for his final assignment. Additionally, the author expresses sincere appreciation to Mr. Humbang Purba, a co-author as well, and the agency supervisor, for his valuable time and knowledge shared throughout the author's journey in completing this work.

GLOSSARY OF TERMS

Definition	Symbol
Gross Depositional Environment (GDE)	
Barrel of Oil Per Day (BOPD)	
Gamma Ray (GR)	
time	ms
depth	ft

REFERENCES

Aldrich, J.B., Rinehart, G.P., Susandhi, R., Schuepbach, M.A. (1995). Paleogene Basin Architecture of the Sunda and Asri Basins and Associated Non-Marine Sequence Stratigraphy.

Bishop, M. G. (2000). Petroleum systems of the northwest Java Province, Java and offshore southeast Sumatra, Indonesia. US Department of the Interior, US Geological Survey.

Clements, B., & Hall, R. (2007). Cretaceous to Late Miocene Stratigraphic and Tectonic Evolution of West Java. Proceedings of the Indonesian Petroleum Association, 31st Annual Convention and Exhibition. Indonesian Petroleum Association, Jakarta, Indonesia.

Kendall, C. (2005). Hand-out Stratigraphy & Sedimentary Basin. Sequence Stratigraphy–Basics, unpublished.

Koesoemadinata, R. P. (2004). Regional Setting of The Sunda and Asri Basins. Jakarta: CNOOC SES Ltd.

Lelono, E. B. (2005). Penelitian Palinologi pada Sedimen Paleogen di Kawasan Indonesia Bagian Barat. Lembaran Publikasi Minyak dan Gas Bumi (LPMGB), 39(2), 15-23. https://doi.org/10.29017/LPMGB.39.2.734.

Lelono, E. B., Irwansyah, I., & Panuju, P. (2011). The Jurassic-Cretaceous Paleogeography Of The Sula Area, North Maluku. Scientific Contributions Oil and Gas, 34(1), 67-83. https://doi.org/10.29017/SCOG.34.1.793.

Metcalfe, I. (2017). Tectonic evolution of Sundaland. Bulletin of the Geological Society of Malaysia. 63. 27-60. 10.7186/bgsm63201702.

Omoboriowo, A.O., Chiaghanam, O.I., Chiadikobi, K.C., Oluwajana, O.A., Soronnadi Ononiwu, C.G. & Ideozu, R.U. (2012). Reservoir characterization of Konga Field, Onshore Niger Delta, Southern Nigeria. International Journal of Emerging Technology 3, 19–30.

Pasaribu, D., Sapiie, B., & Gunawan, I. (2025). Structure Evolution and Palinspastic Analysis of The Gurami-Tamiang Area, North Sumatra Basin, Indonesia. Scientific Contributions Oil and Gas, 48 (3) pp. 341-365. DOI org/10.29017/scog.v48i3.1806.

Ralanarko, D., Wahyuadi, D., Nugroho, P., Rulandoko, W., Syafri, I., Abdurokhim, A., Nur, A. (2021). Seismic Expression of Paleogene Talangakar Formation – Asri & Sunda Basins, Java Sea, Indonesia. Berita Sedimentologi.

Reminton, C. H., & Pranyoto, U. (1985). A hydrocarbon generation analysis in Northwest Java Basin using Lopatin's method. Proceedings of the 14th Annual Convention Indonesian Petroleum Association, v. 2, p. 122-141.

Roksandic, M. M. (1978). Seismic Facies Analysis Concepts. Geophysical Prospecting 95, 383-398.

Rider, M.H. (1999). Geologic interpretation of well logs. Whittles Publishing Services.

Siringoringo, L. P. (2025). High Heat Flow and Geothermal Opportunities in the Sunda Basin, Indonesia: A Case for Sustainable Energy Development. Geological Journal.

Tapponnier, G. P., Peltzer, A. Y. Le Dain, R. Armijo, P. Cobbold. (1982). Propagating extrusion tectonics in Asia: New insights from simple experiments with plasticine. Geology 1982

Todd, D.F., & Pulunggono, A. (1971). The Sunda basinal areas. American Association of Petroleum Geologists Conference, Houston.

Widarsono, B. (2011). Rock Wettability Characteristics Of Some Indonesian Limestones Case Study: Baturaja Formation. Scientific Contributions Oil and Gas, 34(2), 105–116. https://doi.org/10.29017/SCOG.34.2.796.

Wight, A., Sudarmono, & Imron, A. (1986). Stratigraphic Response to Structural Evolution in a Tensional, Back-Arc Setting and Its Exploratory Significance: Sunda Basin, West Java Sea. Jurnal Publikasi IPA (Indonesian Petroleum Association), Vol. 1, pp. 77-100.